This is the accepted manuscript made available via CHORUS. The article has been published as:

Spin-incoherent liquid and interaction-driven criticality in the one-dimensional Hubbard model

Jia-Jia Luo, Han Pu, and Xi-Wen Guan

Phys. Rev. B **107**, L201103 — Published 4 May 2023

DOI: 10.1103/PhysRevB.107.L201103

Spin incoherent liquid and interaction-driven criticality in 1D Hubbard model

Jia-Jia Luo,[1,2] Han Pu,[3,*] and Xi-Wen Guan[1,4,5,†]

[1] *State Key Laboratory of Magnetic Resonance and Atomic and Molecular Physics, Wuhan Institute of Physics and Mathematics, APM, Chinese Academy of Sciences, Wuhan 430071, China*
[2] *University of Chinese Academy of Sciences, Beijing 100049, China.*
[3] *Department of Physics and Astronomy, and Rice Center for Quantum Materials, Rice University, Houston, Texas 77251-1892, USA*
[4] *NSFC-SPTP Peng Huanwu Center for Fundamental Theory, Xi'an 710127, China*
[5] *Department of Theoretical Physics, Research School of Physics and Engineering, Australian National University, Canberra ACT 0200, Australia*

(Dated: April 27, 2023)

Although the one dimensional (1D) repulsive Fermi-Hubbard model has been intensively studied over many decades, a rigorous understanding of many aspects of the model is still lacking. In this work, based on the solutions to the thermodynamic Bethe ansatz equations, we provide a rigorous study on the following: (1) We calculate the fractional excitations of the system in various phases, from which we identify the parameter regime featuring the spin incoherent Luttinger liquid (SILL). We investigate the universal properties and the asymprotic of correlation functions of the SILL. (2) We study the interaction-driven phase transition and the associated criticality, and build up an essential connection between the Contact susceptibilities and the variations of density, magnetization and entropy with respect to the interaction strength. As an application of these concepts, which hold true for higher dimensional systems, we propose a quantum cooling scheme based on the interaction-driven refrigeration cycle.

One-dimensional (1D) Fermi-Hubbard model, describing strongly correlated electrons in a 1D lattice, has become increasingly important in ultracold atoms, condensed matter and quantum metrology. Owing to the Bethe ansatz exact solution of the model [1, 2], a variety of strongly correlated many-body phenomena have been extensively studied for over forty years, including Tomonaga-Luttinger liquid (TLL) [3–5], spin-charge separation [6–9], thermal and magnetic properties [10–16], the Fulde-Ferrell-Larkin-Ovchinnikov (FFLO) [17, 18] pairing correlation [19–24], etc. On the experimental side, 1D exactly solvable models have been successfully realized in the lab, allowing us to compare elegant and sophisticated exact solutions directly with experimental measurements [25–28], Significant new experimental developments cover a broad range of physics such as the generalized hydrodynamics [29–31], dynamical fermionization [32], TLL [33–35], fractional exclusion statistics [36], quantum holonomy [37, 38], p-wave interacting fermions [39–41], high spin symmetry magnetism [42, 43], etc.. For a recent review, see Ref. [44].

Despite of these tremendous efforts, many aspects of the model still lack rigorous understanding. In particular, phase transitions have been extensively studied in the context of varying external potentials such as chemical potential and magnetic field. However, interaction-driven phase transitions have not received sufficient attention even though interaction plays an essential role in many-body systems. Although there are some previous studies along this line (see, for example, Ref. [45–47]), the important quantum critical scaling functions for interaction-driven phase transitions have not been systematically studied. This can be attributed to the fact that interaction strength is hardly tunable in traditional solid materials. The advent of cold atoms completely changed this situation as interaction strengths in atomic systems have been routinely controlled via Feshbach resonance. A notable recent example is the demonstration of the spin-charge separation [48–52] in a 1D continuum Fermi gas where the spin and the charge velocities are shown to exhibit distinct dependence on the interaction strength [53].

Motivated by this, in this Letter, we show that the tunability of interaction strength allows further exploration of the spin incoherent Luttinger liquid (SILL) [54–57] and interaction-driven quantum phase transitions in the Hubbard model. Specifically, we present rigorous results of fractional charge and spin excitations, analytical results on the asymptotic of single-particle Green's function and pair correlation functions of the SILL, and interaction-driven criticality. Furthermore, inspired by the notion of the partial wave Contact in ultracold Fermi gas [58, 59], we build up general relations between Contact susceptibilities and the variation of density, magnetization and entropy with respect to the interaction strength, using which we propose a quantum cooling scheme based on the interaction-driven refrigeration cycle.

1D Hubbard model – The 1D single-band Hubbard

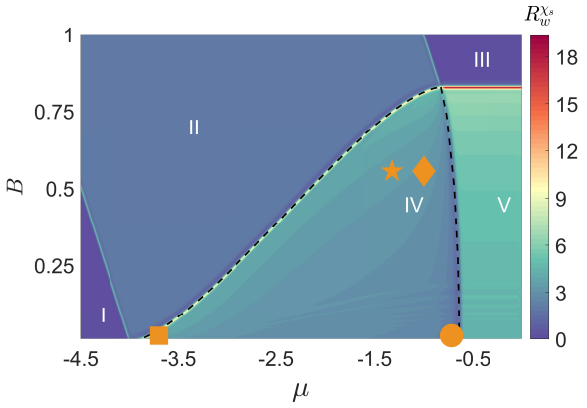


FIG. 1. Phase diagram represented by the contour plot of the Wilson ratio $R_w^{\chi_s}$ at temperature $T = 0.005$ and $u = 1$. The corresponding phases are: empty lattice I, partially filled and fully-polarized phase II, fully-filled and -polarized phase III, partially-filled and -polarized phase IV, and fully-filled and partially-polarized phase V (Mott insulator). The dotted lines represent analytic solution of BA equations obtained at zero temperature. The orange symbols indicates the locations of excitations plotted in Fig. 2.

model is described by the Hamiltonian [1, 5]

$$H = -t\sum_{j=1,a=\uparrow,\downarrow}^{L}\left(c_{j,a}^{\dagger}c_{j+1,a} + \text{h.c.}\right) + u\sum_{j=1}^{L}\left(2n_{j,\uparrow}-1\right)\left(2n_{j,\downarrow}-1\right) - \mu\hat{n} - 2B\hat{S}^{z}, \quad (1)$$

where $c_{j,a}^{\dagger}$ ($c_{j,a}$) is the creation (annihilation) operator of an electron with spin a ($a =\uparrow$ or $\downarrow$) at site j on a 1D lattice of length L, satisfying the standard anticommutation relations. t, μ and B are hopping amplitude, chemical potential and magnetic field, respectively. In this work, we will only consider repulsive interaction with $u > 0$ and take $t = 1$ as the unit of the system. μ and B are renormalized accordingly and become dimensionless. Meanwhile $n_{j,a} = c_{j,a}^{\dagger}c_{j,a}$ and $\hat{n} = \frac{\hat{N}}{L} = \frac{1}{L}\sum_{j,a} n_{j,a}$ are the density operator and the average fermion number per lattice site, respectively. We denote the magnetization $\hat{S}^z = \sum_j \left(n_{j,\uparrow} - n_{j,\downarrow}\right)/2$. For vanishing external potentials ($\mu = 0$, $B = 0$) and even L, Hamiltonian (1) possesses $SO(4) \cong SU(2)\times SU(2)/\mathbb{Z}_2$ symmetry, preserving spin rotational and η-pairing symmetries [5, 61, 62], i.e. $[H, S^{\alpha}] = 0 = [H, \eta^{\alpha}]$ with $\alpha = x, y, z$. The spin and η-pair operators can be transformed to each other via Shiba transformation, showing the connection between spin and charge [5], also see Supplementary Materials [65]. We will use spin and η-pair magnetizations S^z, $\eta^z = \frac{1}{2}(N - L)$ to characterize the fractional spin and charge excitations.

In 1968 Lieb and Wu [1] derived the BA equations for the 1D Hubbard model by means of Bethe's hypothesis [60]. Takahashi [63] later found the root patterns of the BA equations, i.e. real k, length-n Λ string (known as spinon bound state) composed of n spin-down electrons, length-m k-Λ string containing m down-spin and m up-spin particles, which determine both the ground and the excited states of the model. Building on Takahashi's string hypothesis, and using the Yang-Yang method [64], one can obtain the thermodynamic Bethe ansatz (TBA) equations of the model [63] (for convenience, see [65]). In principle, all thermodynamic properties of the model can be obtained from the TBA. However, solving the infinite number of nonlinear integral TBA equations poses a tremendous theoretical challenge. Therefore many important questions remain to be answered.

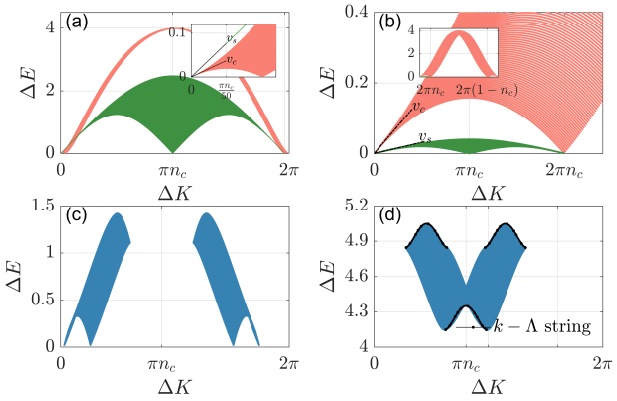


FIG. 2. Elementary fractional spin and charge excitations. The orange areas in (a) and (b) represent particle-hole excitations of charge, whereas the green parts show the two-spinon excitations with quantum numbers $(\Delta\eta^z, \Delta S^z) = (0, 1)$ induced from spin flipping. The inset in (a) shows the excitation for small momentum. While the inset in Fig. (b) shows the excitation for the momentum within the first Brillouin zone, whose zero energy modes are situated at $0, 2\pi n_c, 2\pi(1 - n_c), 2\pi$. (c) Fractional antiholon-spinon excitations $(\frac{1}{2}, -\frac{1}{2})$, i.e. adding an extra spin-down electron to create an antiholon and a spinon. (d) Gapped excitation spectra for length-1 k-Λ string and a length-2 Λ string. All graphs are drawn in the first Brillouin zone with interaction $u = 1$ and the parameters (a): $B = 0, \mu = -0.6619$, density $n = 0.9801$ (near half-filled band); (b): $B = 0, \mu = -3.8508$, density $n = 0.1389$ (dilute limit); (c): $B = 0.555, \mu = -1$; (d): $B = 0.555, \mu = -1.32$.

Low-temperature phase diagram and fractional excitations – A rich phase diagram of the 1D Hubbard model (1) in magnetic field-chemical potential plane can be obtained from either the BA or the TBA equations at zero temperature. We find that the dimensionless Wilson ratio (WR) $R_w^{\chi_s} = \frac{4}{3}\left(\frac{\pi k_B}{\mu_B g}\right)^2 \frac{\chi_s}{C_v/T}$, where χ_s is the spin susceptibility and C_v the specific heat, conveniently characterizes the TLLs. Here k_B, μ_B and g are the Boltzmann constant, the Bohr magneton and the Landé factor, respectively, which we set to be unity in our calculation. The value of the WR is temperature independent at low

energy and exhibits a sudden change in the vicinities of the phase boundaries. Such finite temperature feature naturally maps out the full phase diagram of the 1D repulsive Hubbard model at zero temperature, as we show in Fig. 1. Specifically, we observe that the values of the WR in Fig. 1 confirm the bosonization result [56], i.e. $R_w^{\chi_s} = 2v_cK_s/(v_s+v_c)$, 2 and $4K_s$ for the TLLs in Phase IV, II and V, respectively, where K_s is the Luttinger parameter for spin, $v_{c,s}$ are sound velocities for charge and spin, respectively. The WR is zero for Phases I and III, see SM [65] for more details.

Figure 2 (a) and (b) demonstrate excitations at zero magnetic field in charge and spin degrees of freedom near the half-filled lattice and the dilute limit, respectively. The particle-hole excitation of charge (orange) forms continuum spectra within the first Brillouin zone. Flipping one spin leads to excitation spectrum (green) of two deconfined spinons with a fractional spin-$\frac{1}{2}$. In the long wavelength limit, i.e. $\Delta K \to 0$, both charge and spin excitations exhibit linear dispersion: $\Delta E_{c,s} = v_{c,s}\hbar|\Delta K|$, where $v_c = 0.5995, v_s = 1.2403$ in (a) and $v_c = 0.7206, v_s = 0.1454$ in (b), showing spin and charge separated excitations. However, subtle differences between these two limits are observed, i.e. for (a), the charge excitation displays a single-particle nature due to the vanishing of the charge Fermi sea; for (b), the spin and charge excitations are significantly separated, making this preferred region to observe spin-charge separation [65]. Later, we will further demonstrate the existence of the SILL in region (b) for temperature $E_s \ll k_BT \ll E_F$, where $E_{s,c} \sim k_Fv_{s,c}$ with $k_F = \pi n_c$ are the spin and charge energies, respectively. Fig. 2(c) shows the fractional antiholon-spinon excitation spectra with the η-pair and spin magnization $(\Delta\eta^z, \Delta S^z) = (\frac{1}{2}, -\frac{1}{2})$ by adding an antiholon particle $N_e = N+1$ superposed with one spinon particle in M_1 sector, which are outside of the spin-charge separated TLL regime [65]. Fig. 2(d) shows the two gapped excitations, i.e., length-1 k-Λ string and length-2 Λ spinon bound states, forming a gapped continuum band.

Universal scaling laws, SILL, correlation functions – Rigorous results on quantum criticality of the repulsive Hubbard model remain largely unknown. At zero temperature, the phase transition occurs at a quantum critical point (QCP) where a degree of freedom appears, disappears or reaches saturation. At finite temperature, the QCP fans out into the V-shaped quantum critical regime, in which the free energy takes universal form. By considering the relevant degrees of freedom, we can simplify the TBA equations and find such universal forms. In the SM [65], we have derived analytically the free energies of all quantum critical regions associated with various phase transitions of the 1D Hubbard model. Here, we only write down the free energy at quantum criticality for the II-IV and V-IV transitions:

$$f = f_0 - \frac{\pi T^2}{6v_c} + T^{\frac{3}{2}}\pi^{\frac{1}{2}}\sigma_1(0)\left(\frac{\varepsilon_1''(0)}{2}\right)^{-\frac{1}{2}}\mathrm{Li}_{\frac{3}{2}}\left(-\mathrm{e}^{\frac{-\varepsilon_1(0)}{T}}\right),$$
$$f = f_0 - \frac{\pi T^2}{6v_s} + T^{\frac{3}{2}}\pi^{\frac{1}{2}}\rho(\pi)\left(\frac{-\kappa''(\pi)}{2}\right)^{-\frac{1}{2}}\mathrm{Li}_{\frac{3}{2}}\left(-\mathrm{e}^{\frac{\kappa(\pi)}{T}}\right) \quad (2)$$

where Li_n denotes the polylog functions, f_0 is the ground-state energy, the T^2 terms represents the contributions from the collective excitations of the background degree of freedom near the QCP, $\sigma_1(0)$ denotes the spin density at $\Lambda = 0$, $\varepsilon_1(\Lambda)$ is the dressed energy of length-1 string, and $\varepsilon_1''(0) \equiv \frac{d^2\varepsilon_1}{d\Lambda^2}\Big|_{\Lambda=0}$, $\rho(\pi)$ denotes the charge density at $k = \pi$ and $\kappa''(\pi) \equiv \frac{d^2\kappa}{dk^2}\Big|_{k=\pi}$. with

$$\begin{aligned}\varepsilon_1(0) &= -\ \alpha_B\Delta B - \alpha_\mu\Delta\mu - \alpha_u\Delta u,\\ \kappa(\pi) &= \beta_B\Delta B + \beta_\mu\Delta\mu + \beta_u\Delta u,\end{aligned} \quad (3)$$

denoting the spin dressed energy gaps away from the QCP, where $\Delta B = B - B_c$, $\Delta\mu = \mu - \mu_c$, $\Delta u = u - u_c$ are distances away from the QCP (B_c, μ_c, u_c). The analytic expressions of the factors $\alpha_{B,\mu,u}$ are rather cumbersome and can be found in the SM [65]. As we will show below, the free energy in Eq. (2) elegantly leads to and provides a rigorous understanding of the universal thermodynamic properties of the TLL, the SILL and the quantum scaling laws at criticality.

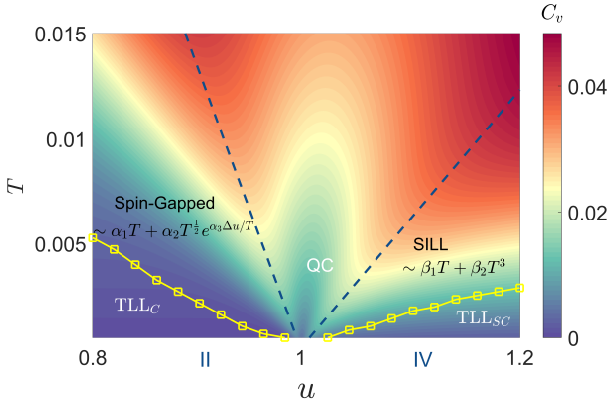


FIG. 3. Contour plot of specific heat in the T-u plane at $\mu = -2, B = 0.55$ for II-IV transition. The blue dashed lines present the critical temperatures determined by the maximum values of the specific heat (Eq.(4)). The yellow lines with square symbols mark the TLL phase boundary, below which the specific heat shows a linear temperature dependence. Crossover regimes between the blue dashed and the yellow lines denote the spin-gapped phase (on the left) and the SILL phase (on the right).

In the quantum critical regime, $T \gg \Delta u$, and from Eq. (2), the specific heat can be readily derived as

$$C_v/T = c_0 + c_1T^{-1/2}\left[\frac{3}{4}\mathrm{Li}_{\frac{3}{2}}(-\mathrm{e}^x) - x\mathrm{Li}_{\frac{1}{2}}(-\mathrm{e}^x) + x^2\mathrm{Li}_{-\frac{1}{2}}(-\mathrm{e}^x)\right] + O((\Delta u/T)^{5/2}), \quad (4)$$

where $x \equiv \alpha_u \Delta u/T$, and $c_{0,1}$ denote the regular part and a constant depending on the critical point u_c, respectively. In Fig. 3, we display the contour plot of the specific heat in the plane spanned by T and u at $\mu = -2$, $B = 0.55$. The specific heat shows a bimodal structure, whose local maxima mark the crossover temperatures. The local maxima can be determined by $\partial C_v/\partial u = 0$, leading to $x_1 = -1.5629$ and $x_2 = 3.6205$, corresponding to the two blue dashed lines in Fig. 3. These two lines join at $u_c = 1$ at $T = 0$ and the quantum critical regime resides between them, displaying a universal free fermion criticality, i.e. dynamical and correlation critical exponents $Z = 2$, $\nu = 1/2$, respectively.

The yellow line with square symbols in Fig. 3 represents the boundary of the TLL region which lies below the line. In the TLL, C_v is linear in T. To the left of u_c, the TLL (labelled as TLL_C) contains only the charge component and $C_v = \frac{\pi}{3}\frac{T}{v_c}$. To the right of u_c, the TLL (label as TLL_{SC}) contains both the spin and the charge component with $C_v = \frac{\pi}{3}\left(\frac{1}{v_c} + \frac{1}{v_s}\right)T$. This is the regime where spin-charge separation [48–52] can be observed. Above TLL_C, the spin sector is gapped and the specific heat is given by $C_v \approx \alpha_1 T + \alpha_2 T^{1/2} \mathrm{e}^{\alpha_3 \Delta u/T}$, where $\alpha_{1,2,3}$ are constants. By contrast, above TLL_{SC}, we find a region of SILL in the temperature range given by $k_F v_s \ll k_B T \ll k_F v_c$, exhibiting a propagating charge mode but not a spin mode with the corresponding specific heat $C_v \approx \beta_1 T + \beta_2 T^3$ with $\beta_{1,2}$ being constants [65], showing a gas-liquid coexistence in the SILL.

In the SILL regime, the spin excitation is suppressed and hence the spin sector is non-dynamic, while charge maintains relevant at low energy. Taking the reasonable limits $|x \pm iv_c t| \ll v_c/T$ and $|x \pm iv_s t| \gg v_s/T$, we can calculate the finite-temperature single-particle Green's function and pair correlation function

$$\begin{aligned} G^{\uparrow} &\approx \mathrm{e}^{-\mathrm{i}k_{F,\uparrow}x}\mathcal{C}_{\uparrow}^{-}(x - \mathrm{i}v_c t)\,\langle S_R^{+}(x,t)\,S_R(0,0)\rangle + h.c., \\ G^{p} &\approx \mathrm{e}^{-\mathrm{i}\left(k_{F,\uparrow}+k_{F,\downarrow}\right)x}\mathcal{C}_{p}^{-}(x - \mathrm{i}v_c t)\,\mathcal{C}_{p}^{+}(x + \mathrm{i}v_c t) \\ &\quad \times\langle S_R^{+}(x,t)\,S_R(0,0)\rangle + h.c., \end{aligned} \tag{5}$$

where the charge correlations $\mathcal{C}_{\uparrow}^{-}(Z) \sim 1/Z^{2\Delta_c^{+}}$, $\mathcal{C}_{p}^{\pm}(Z) \sim 1/Z^{2\Delta_c^{\mp}}$ decay as a power-law of distance, whereas the spin mode correlation $\langle S_R^{+}(x,t)\,S_R(0,0)\rangle \sim (2\pi\alpha k_F)^{2\Delta_s^{+}+2\Delta_s^{-}}\,\mathrm{e}^{-\pi\alpha\left(2\Delta_s^{+}+2\Delta_s^{-}\right)k_F x}$ decays exponentially. Here $\Delta_c^{\pm}$ are the conformal dimensions which can be calculated analytically and numerically [65], α is a constant. For the particular case $B = 0$, our results agree with those given in Ref. [57]. We comment that the SILL has been theoretically studied under the framework of bosonization [55–57]. Our work here provides a rigorous underpinning of the SILL based on the TBA.

Contact susceptibilities and quantum cooling – In analogy to the Contact for quantum gases [58, 59], here we define the lattice version of the Contact $C = \partial f/\partial u = 4d - 2n + 1$, where $n = \langle \hat{n} \rangle$, and $d = \frac{1}{N}\sum_i \langle n_{i,\uparrow} n_{i,\downarrow}\rangle$ is the average double occupancy, a quantity which can also depict the phase diagram [65]. It is, however, more essential to define Contact susceptibilities with respect to the external potentials. Using the Maxwell relations, we may build up general relations between Contact susceptibilities and interaction-driven variations of entropy, density and magnetization [65]:

$$\frac{\partial s}{\partial u} = -\frac{\partial C}{\partial T}, \quad \frac{\partial n}{\partial u} = -\frac{\partial C}{\partial \mu}, \quad \frac{\partial m}{\partial u} = -\frac{\partial C}{\partial (2B)}. \tag{6}$$

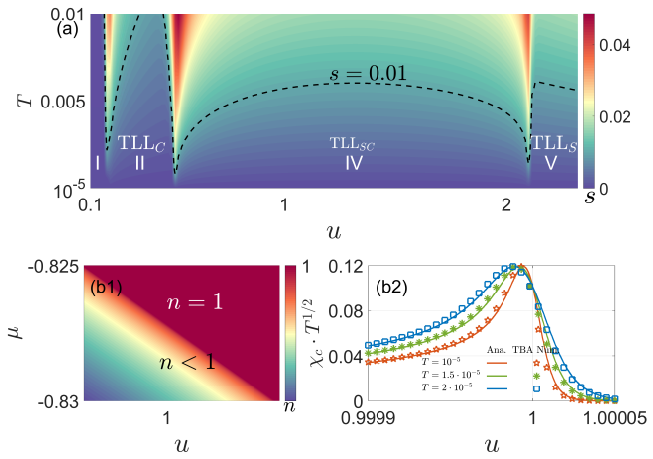


FIG. 4. (a) Contour plot of the entropy in $T - u$ plane for $B = 0.15$, $\mu = -2.5$. Black dotted curve is the isentropic line for $s = 0.01$. When the interaction increases, the system enters sequentially into Phases II, IV and V. (b1) Contour plot of density n near the IV-V phase transition with $u = 1$, $\mu = -0.82724$ and $B_c = 0.82714$. (b2) Scaling behaviour of charge susceptibilities near phase transition from IV to V driven by interaction.

These relations provide deep insights into the interaction effects and universal behaviour of phase transitions.

As a specific example, we now use the first relation in Eqs. (6) to investigate interaction-driven quantum cooling. Fig. 4 (a) shows a contour plot of entropy in the T-u plane for fixed B and μ. The interaction-driven phase transitions from I to II, II to IV, and IV to V occur sequentially with increasing interaction strength. We observe a single-component charge TLL_C in II, a spin and charge separated TLL_{SC} in IV, and a spin TLL_S in the Mott phase V. Conducting the total derivative of entropy with respect to the interaction u, the phase points on the isentropic line in the T-u plane admit the relation $\frac{C_v}{T}\frac{\partial T}{\partial u} = \frac{\partial C}{\partial T}$. Thus the interaction-driven Grüneisen parameter [67] defined by $\Gamma_{int} = \frac{u}{C_v}\frac{\partial C}{\partial T}$ quantifies the efficiency of interaction-driven refrigeration. Near a critical point, local maximum of the entropy leads to a local temperature minimum in an isentropic process, and using the condition $\frac{\partial C}{\partial T} = 0$, we have $\frac{1}{2}\mathrm{Li}_{\frac{1}{2}}(-\mathrm{e}^x) - x\mathrm{Li}_{-\frac{1}{2}}(-\mathrm{e}^x) = 0$ that gives a general solution $x \equiv: \alpha_u \Delta u/T \approx 1.3117$. Using the free energy Eq. (2), we can obtain the explicit expression of the maximum entropy near the transition point from II to IV $s_{c1} \approx \lambda_1 \pi^{1/2}\sigma_1(0)(\varepsilon_1''(0)/2)^{-1/2}T_{c1}^{1/2}$, where $\lambda_1 = x\mathrm{Li}_{1/2}(-\mathrm{e}^x) - 3/2\mathrm{Li}_{3/2}(-\mathrm{e}^x) \approx 1.3467$. Similarly, for phase transition from the Mott phase V to the phase IV, the maximum entropy is given by $s_{c2} \approx \lambda_1 \pi^{1/2}\rho(\pi)(-\kappa''(\pi)/2)^{-1/2}T_{c2}^{1/2}$. On the other hand, the entropy in the Luttinger liquid phases TTL_C and TTL_S are given by $s_{L1} = \pi T_{L1}/3v_c$ and $s_{L2} = \pi T_{L2}/3v_s$, respectively. Therefore through an interaction-driven refrigeration cycle near phase transitions from II to IV and from V to IV in the T-u plane, we can show that the reachable

minimum temperatures are given by

$$\frac{T_{c1}^{1/2}}{T_{L1}} = \frac{\pi^{1/2}(\varepsilon_1''(0)/2)^{1/2}}{3\lambda_1 v_c \sigma_1(0)}, \quad (7)$$

$$\frac{T_{c2}^{1/2}}{T_{L2}} = \frac{\pi^{1/2}(-\kappa''(\pi)/2)^{1/2}}{3\lambda_1 v_s \rho(\pi)}, \quad (8)$$

respectively. The minimum temperature in the T-u plane is governed by the relation $\alpha_u \Delta u/T \approx 1.3117$ [65]. We remark that efficient cooling in lattice is a significant experimental challenge in ultracold atomic gases, the lack of which poses as a roadblock for realizing some exotic quantum phases.

On the other hand, the other two relations in Eqs. (6) provide essential insights for charge (IV-V) and spin (II-IV) phase transitions, respectively. Using these, we find two useful relations among the parameters $\alpha_{u,\mu,B}$ in Eq. (3)

$$\frac{\alpha_u}{\alpha_\mu} = -\frac{\partial \mu}{\partial u}, \quad \frac{\alpha_u}{\alpha_B} = -\frac{\partial B}{\partial u}, \quad (9)$$

that provide us deep insights into the quantum criticality driven by dynamical interaction and external poentials. For example, Fig. 4(b1) shows the phase transition from Phase IV to the Mott phase V in the $\mu - u$ plane, where $\frac{\partial \mu}{\partial u}$ is the slope along the transition line $n = 1$. From Eq. (9) with fixed $B_c = 0.82714$ around $u_c = 1$, $\mu_c = -0.8272$ in Fig. 4(b1), we may numerically get $\alpha_u \approx -1.9627$. With this and using the scaling form of free energy given in Eq. (2), we can obtain the scaling behaviour of the compressibility in terms of u, which is in excellent agreement with numerical calculation from TBA equations, see Fig. 4(b2).

Summary – We have presented new rigorous results of the 1D repulsive Hubbard model. We focus on the interaction-driven quantum criticality which has been largely ignored in previous studies. We studied the fractional excitations from which the SILL regime is identified and carefully investigated. We introduced several Contact susceptibilities and show how they provide crucial new insights into the system. Finally, we proposed a quantum cooling scheme based on the interaction-driven refrigeration cycle, which can potentially open up new avenues of research in reaching unprecedented low temperatures in lattice quantum gases. We note that some of the key concepts developed here will hold true in higher dimensions.

ACKNOWLEDGEMENT

J.J.L. and X.W.G. are supported by the NSFC key grant No. 12134015, the NSFC grant No. 11874393 and No. 12121004. H.P. acknowledges support from the US NSF (PHY-2207283) and the Welch Foundation (Grant No. C-1669).

* hpu@rice.edu
† xiwen.guan@anu.edu.au

[1] E. H. Lieb and F. Y. Wu, Phys. Rev. Lett. **20**, 1445 (1968).
[2] E. H. Lieb and F. Wu, Phys. A **321**, 1 (2003).
[3] T Giamarchi, *Quantum Physics in One Dimension* (Oxford Science Publications, New York, 2004).
[4] A. Imambekov, T. L. Schmidt, and L. I. Glazman, Rev. Mod. Phys. **84**, 1253 (2012).
[5] F. H. L. Essler, H. Frahm, F. Göhmann, A. Klümper and V. E. Korepin, *The One-Dimensional Hubbard Model* (Cambridge University Press, Cambridge, 2005).
[6] M. Boll, T. A. Hilker, G. Salomon, A. Omran, J. Nespolo, Pollet L, I. Bloch, and C. Gross, Science **353**, 1257 (2016).
[7] T. A. Hilker, G. Salomon, F. Grusdt, A. Omran, M. Boll, E. Demler, I. Bloch, and C. Gross, Science **357**, 484 (2017).
[8] J. Vijayan, P. Sompet, G. Salomon, J. Koepsell, S. Hirthe, A. Bohrdt, F. Grusdt, I. Bloch, and C. Gross, Science **367**, 186 (2020).
[9] B. M. Spar, E. Guardado-Sanchez, S. Chi, Z. Z. Yan and W. S. Bakr, Phys. Rev. Lett. **128**, 223202 (2022).
[10] V. Ya. Krivnov and A. A. Ovchinnikov, Zh. Eksp. Teor. Fiz. **67**, 1568 (1974).
[11] N. M. Bogoliubov and V. E. Korepin, Int. J. Mod. Phys. B **3**, 427 (1989).
[12] F. Woynarovich and K. Penc, Z. Phys. B **85**, 269 (1991).
[13] K. Lee and P. Schlottmann, Phys. Rev. B **38**, 11566 (1988).
[14] F. Woynarovich, J. Phys. C **16**, 6593 (1983).
[15] P. D. Sacramento, J. Phys.: Condens. Mat. **7**, 143 (1995).
[16] F. H. L. Essler and V. E. Korepin, Nucl. Phys. B **426**, 505 (1994).
[17] P. Fulde and R. A. Ferrell, Phys. Rev. **135**, A550 (1964).
[18] A. I. Larkin and Y. N. Ovchinnikov, Zh. Eksp. Teor. Fiz. **47**, 1136 (1964).
[19] K. Yang, Phys. Rev. B **63**, 140511(R) (2001).
[20] M. Tezuka and M. Ueda, Phys. Rev. Lett. **100**, 110403 (2008).
[21] A. E. Feiguin and F. Heidrich-Meisner, Phys. Rev. B **76**, 220508(R) (2007).
[22] J. Kajala, F. Massel and P. Törmä, Phys. Rev. A **84**, 041601(R) (2011).
[23] S. Cheng, Y.-C. Yu, M. T. Batchelor and X.-W. Guan, Phys. Rev. B **97**, 121111(R) (2018).
[24] S. Cheng, Y.-Z. Jiang, Y.-C. Yu, M. T. Batchelor and X.-W. Guan, Nucl. Phys. B **929**, 353 (2018).
[25] M. A . Cazalilla, R. Citro, T. Giamarchi, E. Orignac and M. Rigol, Rev. Mod. Phys. **83**, 1405 (2011).
[26] X. W. Guan, M. T. Batchelor and C. Lee, Rev. Mod. Phys. **85**, 1633 (2013).
[27] M. T. Batchelor, and A Foerster, J. Phys. A: Math. Theor. **49**, 173001 (2016).
[28] S. I. Mistakidis, A. G. Volosniev, R. E. Barfknecht, T. Fogarty, T. Busch, A. Foerster, P. Schmelcher, N. T. Zinner, arXiv:2202.11071.
[29] T. Kinoshita, T. Wenger and D. S. Weiss, Science **440**, 900 (2006).
[30] T. Langen, S. Erne, R. Geiger, B. Rauer, T. Schweigler, M. Kuhnert, W. Rohringer, I. E. Mazets, T. Gasenzer, and J. Schmiedmyer, Science **348**, 207 (2015).
[31] M. Schemmer, I. Bouchoule, B. Doyon, and J. Dubail, Phys. Rev. Lett. **122**, 090601 (2019).
[32] J. M. Wilson, N. Malvania, Y. Le, Y. Zhang, M. Rigol, D. S. Weiss Science **367**, 1461 (2020).
[33] B. Yang, Y.-Y. Chen, Y. G. Zheng, H. Sun, H. N. Dai, X.-W. Guan, Z. S. Yuan, J.-W. Pan, Phys. Rev. Lett. **119**, 165701 (2017).
[34] T. L. Yang, P. Grišins, Y. T. Chang, Z. H. Zhao, C. Y. Shih, T. Giamarchi and R. G. Hulet, Phys. Rev. Lett.

121, 103001 (2018).
[35] F. Meinert, M. Panfil, M. J. Mark, K. Lauber, J. X. Caux and H. C. Nägerl, Phys. Rev. Lett. **115**, 085301 (2015).
[36] X. B. Zhang, Y. Y. Chen, L. X. Liu, Y. I. Deng, X.-W. Guan, Natl. Sci. Rev. **9**, nwac027 (2022).
[37] E. Haller, M. Gustavsson, M. J. Mark, J. G. Danzl, R. Hart, G. Pupillo, H. C. Nägerl, Science **325**, 1224 (2009).
[38] W. Kao, K. Y. Li, K. Y. Lin, S. Gopalakrishnan, B. L. Lev, Science, **371** 296 (2021)
[39] Y. T. Chang, R. Senaratne, D. Cavazos-Cavazos, and R. Hulet, Phys. Rev. Lett. **125** , 263402 (2020).
[40] D. J. M. Ahmed-Braun, K. G. Jackson, S. Smale, C. J. Dale, B. A. Olsen, S. J. J. M. F. Kokkelmans, P. S. Julienne, and J. H. Thywissen, Phys. Rev. Research **3**, 033269 (2021).
[41] K. J. Jackson, C. J. Dale, J. Maki, K. G. S. Xie, B. A. Olsen, D. J. M. Ahmed-Braun, S. Zhang, J. H. Thywissen, arXiv:2206.10415.
[42] G. Pagano, M. Mancini, G. Cappellini, P. Lombardi, F. Schäfer, H. Hu, X.-J. Liu, J. Catani, C. Sias, M. Inguscio and L. Fallani, Nat. Phys. **10**, 198 (2014).
[43] B. Song, Y. Yan, C. He, Z. Ren, Q. Zhou, and G. B. Jo, Phys. Rev. X **10**, 041053 (2020).
[44] X.-W. Guan and P. He, Rep. Prog. Phys. **85**, 114001 (2022).
[45] H. Chen and K. Yang, Phys. Rev. B **85**, 195113 (2012).
[46] W. Li, D. N. Sheng, C. S. Ting, and Y. Chen, Phys. Rev. B **90**, 081102(R) (2014).
[47] H. Pan, and S. Das Sarma, Phys. Rev. Lett. **127**, 096802 (2021).
[48] F. D. M. Haldane, J. of Phys. C: Solid State Physics, **14**, 2585 (1981).
[49] A. Recati, P. O. Fedichev, W. Zwerger, and P. Zoller, Phy. Rev. Lett. **90**, 020401 (2003).
[50] J.Y. Lee, X.-W. Guan, K. Sakai, and M.T. Batchelor, Phys. Rev. B, **85**, 085414 (2012).
[51] M. Mestyán, B. Bertini, L. Piroli, and P. Calabrese, Phys. Rev. B, **99**, 014305 (2019).
[52] O. I. Pâţu, A. Klümper, and A. Foerster, Phys. Rev. B, **101**, 035149 (2020).
[53] R. Senaratne, D. Cavazos-Cavazos, S. Wang, F. He, Y.-T. Chang, A. Kafle, H. Pu, X.-W. Guan, R. G. Hulet, Science **376**, 1305 (2022).
[54] D. Cavazos-Cavazos, R. Senaratne, A. Kafle and R. G. Hulet, arXiv:2210.06306.
[55] G. A. Fiete, and L. Balents, Phys. Rev. Lett. **93**, 226401 (2004).
[56] G. A. Fiete, Rev. Mod. Phys. **79**, 801 (2007).
[57] V. V. Cheianov and M. B. Zvonarev, Phys. Rev. Lett. **92**, 176401 (2004).
[58] S. Tan, Ann. Phys. **323**, 2952 (2008).
[59] S. Zhang and A. J. Leggett, Phys. Rev. A **79**, 023601 (2009).
[60] H. A. Bethe, Z. Phys. **71**, 205 (1931).
[61] C. N. Yang, Phys. Rev. Lett. **63**, 2144 (1989).
[62] C. N. Yang and S. C. Zhang, Mod. Phys. Lett. B **4**, 759 (1990).
[63] M. Takahashi, Prog. Theor. Phys. **47**, 69 (1972).
[64] C. N. Yang and C. P. Yang, J. Math. Phys. **10**, 1115 (1969).
[65] See Supplemental Material in which we present some key derivations of the results on the fractional excitations, SILL correlation functions, interaction driven criticality and quantum cooling for the 1D repulsive Hubbard model. The Supplemental Material also contains Ref. [66].
[66] N. Mohankumar, Comp. Phys. Commun. **176**, 665 (2007).
[67] Y.-C. Yu, S.-Z. Zhang and X.-W. Guan, Phys. Rev. Research **2**, 043066 (2020).